EEET ECOLOGICAL ENGINEERING & ENVIRONMENTAL TECHNOLOGY

Ecological Engineering & Environmental Technology, 2026, 27(7), 160–174
https://doi.org/10.12912/27197050/222596
ISSN 2719–7050, License CC-BY 4.0

Received: 2026.03.10
Accepted: 2026.06.15
Published: 2026.07.01

Multi-index drought assessment using vegetation and meteorological indicators in the Thabo Mofutsanyane district, South Africa

Lokuthula Msimanga[1*], Sonwabo Perez Mazinyo[1]

[1] Department of Chemical and Earth Sciences: Geography and Environmental Science, University of Fort Hare, Private Bag X1314, Alice, 5700, South Africa
* Corresponding author's e-mail: mlokuthula05@gmail.com

ABSTRACT

This study aims to quantify the frequency, severity, and spatial distribution of agricultural droughts in the Thabo Mofutsanyane district, South Africa, and to assess the relative contributions of precipitation and vegetation conditions to drought impacts. Monthly rainfall data from 1906 to 2023 were analyzed using the standardized precipitation index (SPI) at multiple timescales, while MODIS vegetation indices including the vegetation condition index (VCI), temperature condition index (TCI), and vegetation health index (VHI) were processed in Google Earth Engine for the period 2002–2022, the study identified both long-term trends and localized patterns of drought stress. This multi-index approach enabled the identification of both long-term drought trends and localized vegetation stress patterns. The results reveal that drought frequency has increased over the last century, with extreme events in 1919, 1965, 1992, 2015, and 2018, while the 2018 event affected up to 80% of the district. Vegetation indices highlighted areas of severe local stress as well as pockets of resilience, demonstrating that vegetation responses are not solely determined by precipitation. Correlation analysis revealed strong and statistically significant relationships between VCI and VHI ($r = 0.902$, $p < 0.001$) and between VHI and TCI ($r = 0.886$, $p < 0.001$), while weak and non-significant correlations were observed between SPI6 and vegetation indices, underscoring the role of temperature and vegetation stress. Limitations of the study include the shorter temporal coverage of vegetation indices compared to rainfall records and the absence of socio-economic factors that may influence resilience to drought. The combined analysis of SPI and satellite-derived vegetation indices quantified drought severity across the district, revealing that temperature-driven vegetation stress often intensified drought impacts independently of rainfall anomalies. This study identified specific areas consistently vulnerable to severe droughts, providing a spatially explicit assessment that can directly guide drought risk management and adaptation strategies.

Keywords: MODIS datasets, vegetation health index, standardized precipitation index, Google Earth Engine, spatio-temporal drought analysis, Thabo Mofutsanyane district.

INTRODUCTION

Drought is considered a slow onset climatic phenomenon with consequences that manifest incrementally over time (Hashemzadeh et al., 2022; Nabizada and Köylü, 2025). It is a climatic disaster caused by a lack of rainfall, humidity and increased temperature, deviating from normal climate conditions (Nabizada and Köylü, 2025). Drought classifications include meteorological (precipitation deficit), agricultural(soil moisture deficit), hydrological (reduced river flow and groundwater recharge), and socio-economic drought (impacting human activities and livelihoods) (Mckee et al., 1993; Ncube, 2017). Over time, drought influences water resource availability, vegetation cover, agriculture, food security and subsequently affecting the broader socio-economic environment (Pavlidis et al., 2024; Badasa et al., 2022). Consequently, drought monitoring and assessment require sustained scientific attention (Bhowmik and Bhatt, 2024).

In Africa, recurrent droughts frequently degrade livelihoods and agricultural productivity across numerous ecological regions. For example, the Horn of Africa comprising of east African countries including primarily Somalia, Ethiopia, Eritrea and Djibouti has experienced recurrent droughts since the 1970s, resulting in widespread famine, loss of livelihood and displacement of populations. In addition, the 2015–2016 El Niño-induced drought in Southern Africa affected more than 40 million people and was categorised as one of the region's most severe in decades (FAO, 2017). In South Africa, this El Nino event was declared a national disaster due to its extensive impacts on water supply, agriculture and livelihoods (Baudoin et al., 2017).

Recurrent droughts in past decades have led to substantial economic losses for commercial and small-holder farmers in South Africa. Agricultural activities in the country are predominantly rain-fed, and thus highly susceptible to climate-related risks specifically, increased rainfall variability (Pavlidis et al., 2024). The 1992 drought was recorded as the worst since 1900, resulting in approximately 70% crop failure, livestock deaths, and food insecurity (Mukhawana and Kanyerere, 2023). Some provinces in South Africa have felt the brunt of droughts more than others. Between 2015 and 2018, the Western Cape province, specifically Cape Town experienced severe drought which was declared a national disaster, resulting in strict water rationing and what was widely referred to as the "Day Zero" crisis (Wolski, 2018). The Free State province has also experienced significant socio-economic losses due to prolonged droughts in spite of its status as South Africa's breadbasket due to its vital role in food production and water storage (Adelabu et al., 2025).

Drought assessments in vulnerable but economically viable areas such as the Eastern Free State are particularly important because reliance on rain-fed agriculture further exposes vulnerable local communities to climate variability. Early drought detection can mitigate the negative effects on available water resources and water stress in the agricultural sector (Wyss et al., 2022) through improved planning and implementation of water conservation measures. Human-induced climate change has increased the occurrence and frequency of ecological changes (Kashyap et al., 2025).

Precipitation data scarcity and incomplete datasets undermine data quality resulting in erratic regional drought analysis when using only *in-situ* rainfall data (Pavlidis et al., 2024). Satellite imagery has become a useful tool in drought detection through the use of derived images at various resolutions, allowing for detailed supra-regional time series analysis and monitoring (Wyss et al., 2022). Previous South African studies have applied meteorological indices such as SPI, SPEI, and PDSI to assess drought variability (Mathivha and Matimolane, 2025) (Kganyago et al., 2021). Others have integrated rainfall and vegetation indices, including SPI with NDVI or VCI, to capture both climatic and ecological dimensions of drought (Botai et al., 2016; Hlalele, 2019; Tshabalala, 2023). Vegetation-based indices such as the vegetation condition index (VCI), temperature condition index (TCI), vegetation health index (VHI), land surface temperature (LST), and enhanced vegetation index (EVI) have also been widely used to assess drought conditions in South Africa (Mukhawana and Kanyerere, 2023; Orimoloye et al., 2021). These studies demonstrate that multi-index approaches are established nationally, but few have been applied at the district scale in mountainous regions such as the Eastern Free State, where limited meteorological stations and complex terrain make local monitoring particularly challenging.

Spatial and temporal local analysis of droughts is critical for monitoring, planning and the development of early warning systems (Fentaw et al., 2023). This is true particularly for mountain environments such as the EFSR due to greater altitudinal range, extreme topographical differences, diverse agro-ecological systems, and climate sensitivity. Managing diverse topographies, microclimates, and farming techniques depends on local-level drought analysis for drought risk reduction and sustainable land management planning (Fentaw et al., 2023).

Despite these advances, fewer studies have examined recent environmental changes accelerating the occurrence of agricultural drought in South Africa, particularly within the Thabo Mofutsanyane district of the Free State province. Meteorological droughts are more frequently studied in the Free State with ecological/agricultural droughts remaining relatively unexplored.

Drought indices are not universally applicable across regions, and there is no single index that can represent all aspects of droughts (Mukhawana and Kanyerere, 2023). Their utility is strongly influenced by regional climate (Nabizada and Köylü, 2025) and mountain areas typically have

different microclimates driven by complex topography, varying elevation and aspect. Droughts also vary in intensity, spatial distribution, frequency, and severity across different climatic zones which makes them complex and dynamic (Nabizada and Köylü, 2025).

Previous studies in South Africa have advanced drought monitoring, but have mostly focused on the isolated application of rainfall or vegetation indices (Mukhawana and Kanyerere, 2023) This limits their ability to capture the intricacies associated with drought occurrences. Despite the widespread use of drought indices in the country, limited attention has been given to the comparative performance and sensitivity under heterogeneous environmental conditions. Most existing studies apply individual indices or combine them without critically evaluating their consistency and responsiveness to drought signals.

Drought is a complex and multidimensional phenomenon that cannot be fully captured by a single indicator. While previous studies in South Africa have applied either meteorological or vegetation-based indices, fewer have integrated multiple indicators to provide a comprehensive assessment of both climatic and ecological drought conditions. This study addresses this gap by analysing the spatio-temporal behaviour of multiple drought indices (SPI, EVI, TCI, VCI, and VHI) within the Thabo Mofutsanyane district, with the objective of examining whether the integration of meteorological and vegetation-based indicators provides a more comprehensive representation of drought processes and their impacts. By comparing their responses to drought conditions across time and space, the study provides insights into their relative sensitivity and reliability in capturing agricultural drought dynamics. Consequently, the use of multiple indices to analyse drought provides sounder interpretation of drought impacts than single-parameter indices (Wyss et al., 2022).

Therefore, this study investigates the spatio-temporal dynamics of agricultural drought using remotely sensed data from multiple sources, such as SPI, EVI, TCI, VCI, and VHI in the Thabo Mofutsanyane district of South Africa. The specific objectives of the study are to: (1) analyse the magnitude and frequency of agricultural droughts using VCI, TCI, and VHI; (2) examine the spatial and temporal patterns of meteorological droughts using SPI. This study applies a multi-index approach to drought monitoring at the district scale in the mountainous Free State region, addressing both geographic (local-scale, mountainous terrain) and methodological (multi-index integration) gaps. The purpose of this study is to discover whether integrating meteorological and vegetation-based indicators can reveal previously unknown patterns of resilience and vulnerability across agro-ecological zones, filling a critical gap in district-scale drought monitoring.

MATERIAL AND METHODS

Study area

The study was conducted in the Thabo Mofutsanyane district, located in the Free State province, South Africa. The district is within the Afromontane region, and located between 27°03′ and 29°08′ S and between 119°37′ and 121°26′ E. The district makes up almost a third of the Free State province's geographical area, with an area of 33,269 km^2. Elevation in this region ranges between 1500 and 3000 metres above sea level. The climate is classified as Cwb (temperate oceanic, with dry winters and warm summers) under the Köppen–Geiger system. Mean annual precipitation ranges between 600 and 1200 mm, concentrated during the summer (October–March). Winters are cold with frost and occasional snow, while summer maximum temperatures reaching 28–32 °C (Mukhawana and Kanyerere, 2023; Adelabu et al., 2025).

The spatial boundary of the study area was defined using the administrative boundary shapefile of the Thabo Mofutsanyane district municipality (source: Municipal Demarcation Board of South Africa), and all spatial analyses were constrained to this polygon.

Data collection and analysis

Satellite data

MODIS satellite data were obtained from the Google Earth Engine (GEE) platform for the period 2002–2022 were used to derive the EVI, VCI, TCI and VHI indices. The MOD13Q1 (collection 6.1) product was used to derive the enhanced vegetation index (EVI) at a spatial resolution of 250 m and 16-day temporal resolution. Land surface temperature (LST) data were obtained from the MOD11A2 (Collection 6.1) product at 1 km spatial resolution and 8-day temporal resolution. The LST values were rescaled by a

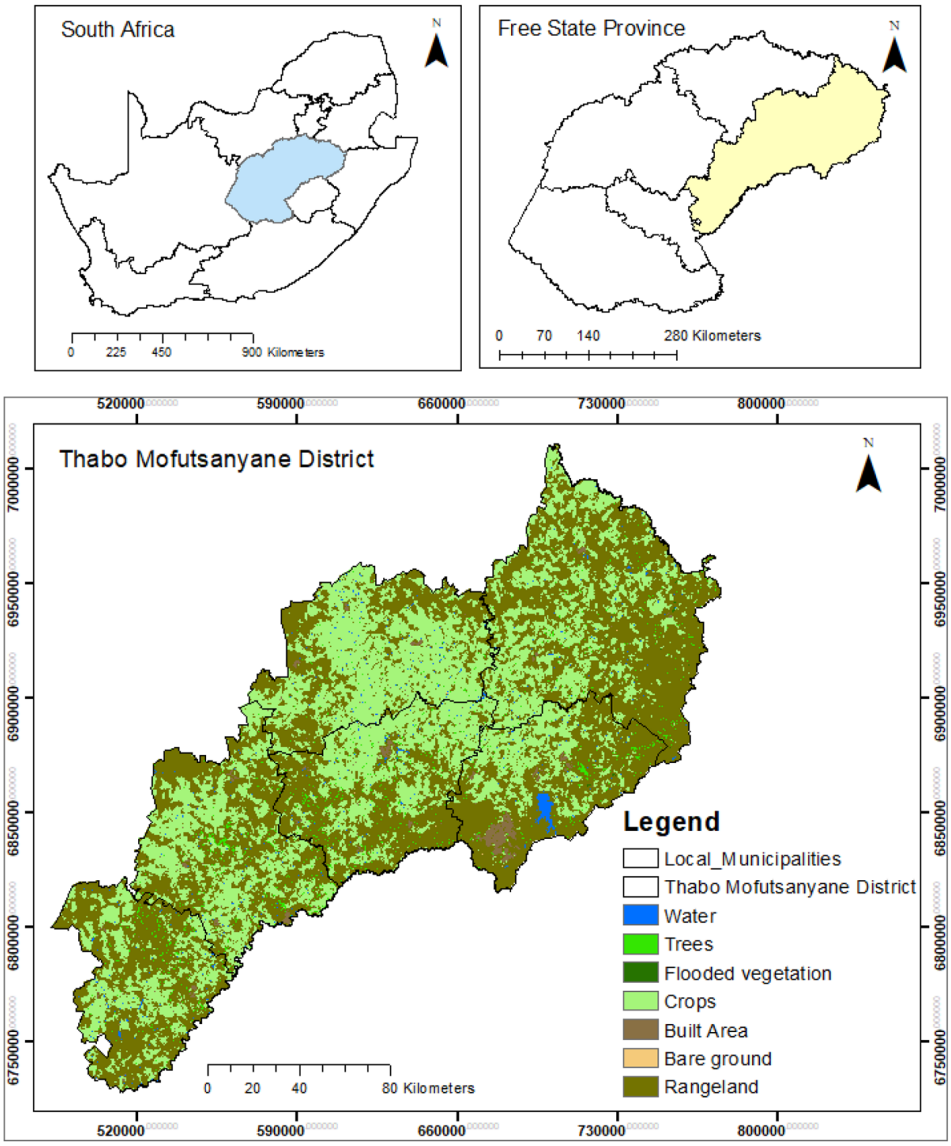

Figure 1. Study area showing land use land cover changes (LULC 2022)

factor of 0.02 and converted into °C to standardize and enhance comparability with atmospheric temperature data. All datasets were resampled to a common spatial resolution of 1 km using bilinear interpolation and reprojected to WGS84. Cloud-contaminated pixels were removed using the quality assurance (QA) flags provided within each MODIS product, explicitly retaining SummaryQA values 0 and 1. Drought indices were calculated for the cropping season (October to March). Monthly composites were generated using mean value compositing to reduce noise and ensure temporal consistency. All preprocessing steps, including filtering, masking, resampling, and index calculation, were implemented in GEE. The full processing workflow is provided in Supplementary Material (Code S3–S5).

Temperature condition index

TCI is a satellite derived metric used to determine vegetation stress resulting from extreme temperatures and excessive moisture (Bhowmik and Bhatt, 2024). LST provides the thermal measurement used to calculate TCI. The vegetation health index (VHI) applied for drought monitoring is found by combining TCI and VCI (Bento, 2018). Higher LST values ultimately increase plant evapotranspiration, reducing accessible surface soil moisture (Bhowmik and Bhatt, 2024). TCI is calculated using the following formula:

$$TCI = \frac{LSTmax - LSTi}{LSTmax - LSTmin} \times 100 \quad (1)$$

LST_i is the observed pixel value of the current month temperature, LST_{max} and LST_{min} are

maximum and minimum surface temperature values respectively. LST_{max} and LST_{min} were calculated per pixel across the entire study period (2002–2022), using the full MOD11A2 record as the climatology baseline. The time scale applied was monthly composites, generated by averaging the 8-day LST values within each month, restricted to the cropping season (October–March). This approach ensures that TCI reflects relative thermal stress compared to each pixel's historical range rather than a single global threshold.

Vegetation condition index

VCI is used to monitor drought and changes in vegetation health. The index also assists in examining how soil moisture and precipitation variables affect vegetation health by focusing on the impacts of moisture on vegetation (Bhowmik and Bhatt, 2024). In this study, EVI was used to calculate VCI instead of the commonly used NDVI. The main reasons for using EVI over NDVI include improving sensitivity, lessening atmospheric interference particularly in canopy dense and high aerosol areas and also offering more stability across different land cover types (Rahimabadi et al., 2024; Adelabu et al., 2025). The VCI was calculated on a monthly temporal scale, using long-term EVI records. The baseline values (*EVImin* and *EVImax*) were derived from the minimum and maximum monthly EVI values observed for each pixel across the entire study period. This ensures that the VCI reflects relative vegetation health compared to its historical range. The VCI is calculated using the following formula (Adelabu et al., 2025),

$$VCI_{ijk} = \frac{EVIijk - EVIi,min}{EVIi,max - EVIi,min} \times 100 \quad (2)$$

where: VCI_{ijk} is the *VCI* value for pixel *i* during month *j* in year *k*. *VCI* values range from 0–100, with higher *VCI* values denoting healthy vegetation and lower values denoting poor vegetation state. In this study, *VCI* values were sub-divided it into five classes (Table 1).

Table 1. Classification ranges for TCI, VCI, and VHI in drought monitoring

Category	No.	VCI, TCI, VHI
Extreme drought	1	<10
Severe drought	2	10–20
Moderate drought	3	21–30
Mild drought	4	31–40
No drought	5	>40

Thresholds follow Adelabu et al. (2025) and Rahimabadi et al. (2024), ensuring comparability with regional drought monitoring studies. While operational thresholds vary across literature, these ranges provide consistency for agricultural drought assessment in South Africa.

Vegetation health index

VHI is a commonly used remote sensing-based agricultural drought index combining vegetation state (VCI) with thermal/moisture stress (TCI) in monitoring drought (Wyss et al., 2022). Simultaneous use of the two indices broadly represents vegetation health and has a more solid relationship with soil moisture than when VCI or TCI are used as single-sensor indices (Wyss et al., 2022).

$$VHI = aVCI + (1\text{-}a)TCI \quad (3)$$

where: *VHI* – vegetation health index, $a = 0.5$ (contribution of VCI and TCI), *VCI* – vegetation condition index, *TCI* – temperature condition index. *VHI* is represented using percentages (0–100%) classified into five groups (Table 1).

The weighting factor (a = 0.5) was adopted following Kogan's original formulation of the *VHI*, which assumes equal contributions of vegetation condition (*VCI*) and thermal stress (*TCI*) to vegetation health. Several studies have applied this balanced weighting to ensure comparability across regions and datasets (Kogan, 1995; Kogan, 1997; Rojas et al., 2011; Wyss et al., 2022).

Standardized precipitation index

SPI exclusively uses precipitation data to spatially and temporally monitor meteorological drought patterns (Fentaw et al., 2023). Monthly rainfall data from 1900–2023 were downloaded from Climate Explorer platform (https://climexp.knmi.nl/), using study area geographic coordinates following the approach of (Msimanga and Mukwada, 2025). The data were obtained from the Climate Research Unit time-series (CRU TS v4.07) at a 0.5°× 0.5° resolution. A total of 34 grid points within the boundaries of the EFSR and those in the immediate surroundings were considered for analysis to represent district-level precipitation. The 1-month (SPI-1), 3-month

(SPI-3), 6-month (SPI-6) and 12-month (SPI-12) time scales were analysed for precipitation anomalies leading to drought occurrence. SPIs were calculated using the gamma distribution method implemented in the SPEI package in RStudio. SPI index values are either positive or negative, with the former indicating wet conditions and the latter indicating dry conditions or episodes. SPI values were categorised into five equal-intervals between −2.0 and +2.0 (1 = extreme dry: −2.0 to −1.2; 2 = moderately dry: −1.2 to −0.4; 3 = near normal: −0.4 to 0.4; 4 = moderately wet: 0.4 to 1.2; 5 = very wet: 1.2 to 2.0). This equal-interval scheme was selected to maintain equal category widths and symmetry around the central zero value. While Copernicus EDO/WMO recommend thresholds at −2.0, −1.5, −1.0, +1.0, +1.5, and +2.0, this adaptation ensures regular category spacing for comparative analysis.

Statistical analysis

To assess long-term changes, Mann–Kendall trend tests and Sen's slope estimator were applied to SPI time series, providing statistical significance for observed drought trends. Statistical significance was evaluated at $p < 0.05$. Spatial interpolation was conducted using ordinary kriging, with a spherical variogram model selected based on lowest RMSE and highest R^2 values during cross-validation. The Pearson correlation coefficient was used to measure the linear correlation between EVI, TCI, VCI, and VHI with SPI6. All analyses were performed in R (version 4.4.1) using the 'trend' package for Mann–Kendall, and Sen's slope tests, and the 'SPEI' package for SPI calculation. Correlation analyses were conducted using the 'corrplot' package.

Study limitation

The study limitations include: (1) The performance of indices relies on a myriad of variables including climate, topography, vegetation type, and soil texture, which were not fully explored in this study. Vegetation analysis using MODIS-based indices (VCI, TCI, VHI) only covered the past two decades, limiting long-term analysis in comparison to SPI. (2) Vegetation indices do not discriminate between natural landscapes and irrigated or managed vegetation patches as the latter may mask drought signals, leading to localised anomalies. (3) The socio-economic vulnerability factors (income, household size, education, employment status, poverty, dependence on natural resources) were not quantitatively assessed, though they strongly influence vegetation health through socio-ecological interactions. Future work should integrate socio-economic vulnerability factors.

RESULTS AND DISCUSSION

Climatic characteristics of Thabo Mofutsanyane district

The average annual rainfall from 1906 to 2023 recorded in the study area was analysed (Figure 1). The results show that the years with the highest recorded rainfall averaging between 900–1036 mm were 1909, 1942, 1943, 1957, 1976, 1996, and 2021. The years 1942 and 1943 were the only two years where high rainfall is consecutively recorded, that is, 942.8 and 1035 mm respectfully. Figure 2 Annual precipitation trends (1901–2023). The Mann–Kendall test revealed a weak, non-significant monotonic trend ($\tau = 0.045$, $p = 0.457$), while Sen's slope estimated a slight decline of −0.261 mm per year, indicating that long-term rainfall variability is largely stable. The years where the highest rainfall was recorded were 1942–43, 1957, 1976, 1996, and 2021. These findings align with previous analyses that highlighted these years as uncharacteristically wet in the Free State province (Kruger and Nxumalo, 2017; McBride et al., 2022). The lowest rainfall was recorded in the years 1919 (481.9 mm), 1965 (478.5 mm), 1992 (456.2 mm) and 2015 (452 mm). Rainfall values reflected in 1992 and 2015 corroborate with the well-documented El Niño-induced drought that occurred across Southern Africa during those periods (Rouault et al., 2003; Reason and Jagadheesha, 2014). Other studies also concurred that 1992 and 2015 were the driest years in South Africa (Blamey et al., 2018; Wolski et al., 2020). The low rainfall recorded in 1965, 1992, and 2015 also aligns with drought episodes in the Free State Province in those years (Botai et al., 2016).

Meteorological drought analysis

SPI values were calculated from 1906 to 2023 at four timescales (1, 3, 6, and 12 months). At the 1-month timescale (SPI-1), the dataset highlighted short-term droughts in August 1902 (SPI –2.76) and April 2015 (SPI < –2.0), confirming these

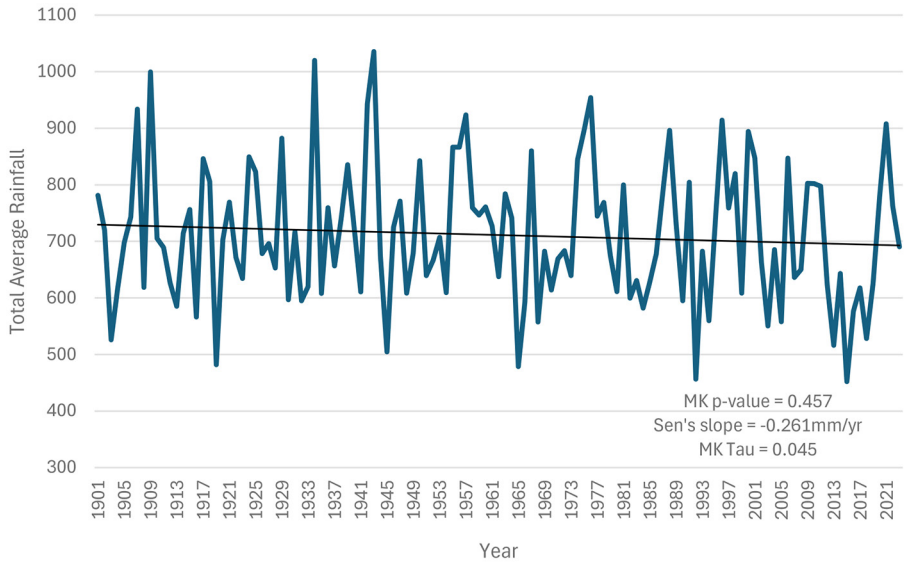

Figure 2. Annual precipitation trends (1901–2023)

months show severe anomalies depicting extremely dry weather. Other series of dry months occurred in 1932–33, 1942–44, 1947–49, 1953–57, 1961–65, 1970–73, 1980–82, 1987, 1992, 2009, and 2019 with SPI-1 values below 1.5 (Figure 3).

The Mann–Kendall test revealed highly significant drying trends in SPI-1, SPI-6, and SPI-12. Sen's slope estimator estimates indicated declines of −0.0002 mm/year (SPI1), −0.0048 mm/year (SPI6), and −0.0003 mm/year (SPI12), confirming statistically significant drying trends. In contrast, SPI3 showed only a weak drying tendency (−0.0045 mm/year), which was not statistically significant ($\tau = -0.031$, $p = 0.053$). This suggests that while longer accumulation periods (SPI6 and SPI12) capture sustained drying signals, short-term variability (SPI3) does not show a robust or significant trend. Higher rainfall was recorded in 1904, 1906, 1907, 1911, 1919, 1923, 1959, 1976, 1996, 2001, 2010–11, 2018, 2021, and 2023 creating wet anomalies with monthly SPI-1 values exceeding +1.5, thus demonstrating extreme rainfall episodes (Figure 3). The driest year recorded was 1984 at the 3-month

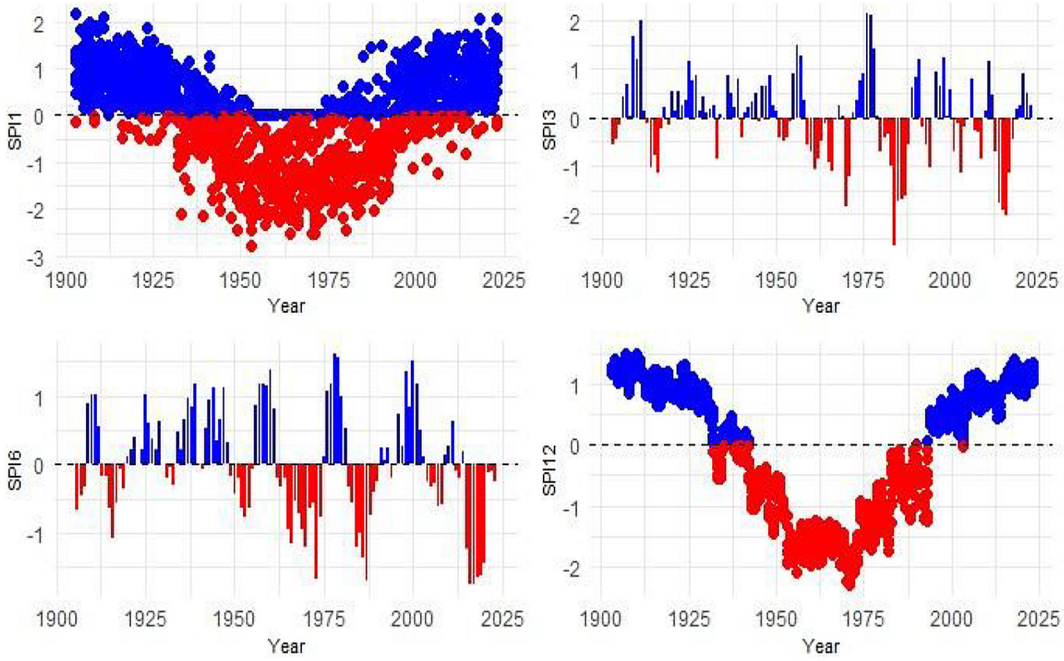

Figure 3. SPI time series at 1, 3, 6, and 12-month scales (1903–2023) for Thabo Mofutsanyane district

time scale with SPI-3 values of –2.72 (June–August) and –3.06 (August–October). The second most severe drought was recorded in 2015, with deficits stretching from July (SPI-3 = –2.34) to August (–1.78) and September (–1.68). In 1987, more severe droughts were recorded with SPI values calculated at the 3-month time scale (SPI-3 = –1.57), 1993 (–1.65), 2009 (–1.68), and 2019 (–1.68). Conversely, high rainfall events were recorded in 1911, 1929, 1941, 1947, 1959, 1977, 1996, 2001, and 2021, with SPI-3 > +1.2 reflecting wet conditions. At the 6-month time scale, prolonged droughts were recorded in 1953, 1965, 1971, 1983, 1989, 2007, 2013, 2018, and 2023. The year 2018 again emerged as experiencing the most severe drought (SPI-6 = < –1.2) in the greater part of the district. On the other hand, high rainfall years included 1911, 1929, 1941, 1947, 1959, 1977, 1996, 2001, and 2021, with SPI-6 values exceeding +1.2, highlighting extensive rainfall surpluses through the growing seasons of those years.

Long-term anomalies reflect prolonged drought and wet periods at the 12-month time scale (SPI-12). High rainfall anomalies were primarily recorded in early rainfall records where SPI-12 values were consistently positive, that is, above +1.2 in 1903–1911 reflecting wet conditions. On the contrary, extreme dry conditions were recorded from 1953–1960 (SPI-12 = –1.9 to –2.0), 1965–1972 (SPI-12 = –2.2), and 1980–1983 (SPI-12 = –1.7), revealing multi-year droughts. Later droughts were detected in 1992 (SPI-12 = –1.23), 2015 (SPI-12 = –1.0), and 2019 (SPI-12 = –1.25), while higher rainfall patterns re-appeared in 2010–2011, 2018, 2021, and 2022, with SPI-12 values surpassing +1.2.

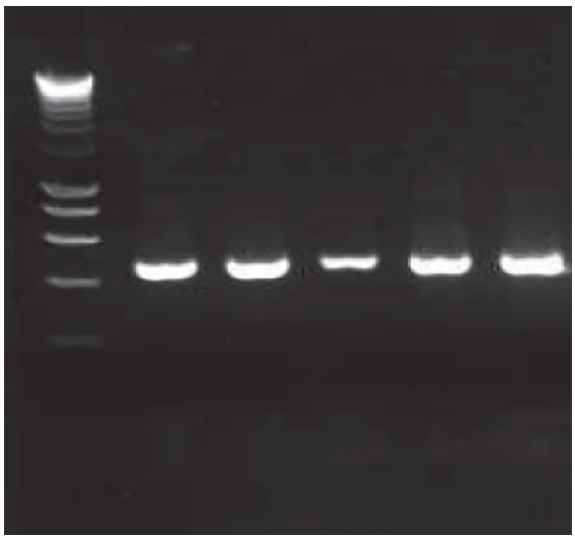

Figure 4. (a) Spatial drought mapping using 6-month SPI from 1906–1965, (b) spatial drought mapping using 6-month SPI from 1971–2023

Spatial drought mapping using 6-month SPI from 1906–2023

The Ordinary Kriging method was used to interpolate the spatial distribution of SPI-6 values in the district (Figure 4a and 4b). The maps show that the intensity and spatial extent of drought occurrences varied across the study area. For example, in 2013 and 2023, the northeast parts of the district recorded severe to moderate droughts, with the central parts remaining around normal (SPI values between -0.4 to + 0.4), while small parts of the southwest district recorded wetter conditions with higher SPI values.

The most severe drought was experienced in 2018 by more than 80% of the district, where SPI values were below -1.2 (extremely dry). Severe to moderate dry spells were also recorded in 1953, 1965, 1971, 1983, 1989 and 2007, affecting 60–70% of the district. These extensive droughts highlight the vulnerability of the district to water stress in those years, which negatively impacted local communities. Studies suggest that the decline in vegetation in most districts is not only a consequence of fewer hectares planted, but adverse weather conditions and the withdrawal of government support (Van Niekerk and Conradie, 2023). Thabo Mofutsanyane District has been experiencing water scarcity problems in the different municipalities (Mukwada and Mutana, 2023; Msimanga and Mukwada, 2024). Compounded stressors increase vulnerability to drought impacts in municipalities and households who lack adaptive capacity and resilience (Adelabu et al., 2025). Therefore, there is an urgent need for local-level drought risk assessment and adaptation planning to minimise future drought hazards (Adelabu et al., 2025). Household socio-economic and demographic characteristics, such as, income, level of education, household size and location can influence resilience to drought-related shocks (Bahta and Myeki, 2021). The district is reported to be highly populated, and also plagued with high poverty and unemployment rates (Statistics South Africa, 2023). Subsequently, socio-economic challenges in the district will likely worsen driven by reoccurring droughts and other climate hazards

(Van Niekerk and Conradie, 2023; Mukwada and Mutana, 2023).

A similar SPI analysis in the Luvuvhu River catchment area, Limpopo, reported the occurrence of extreme droughts during 1982/83, 1991/92 and 2015/16 agricultural seasons (Mazibuko et al., 2021). The current study findings also align with previous research in the northeast and eastern regions of South Africa highlighting persistent droughts over the years and indicating the escalating frequency and intensity of drought events (Kruger and Nxumalo, 2017; Onyeuwaoma, 2024). Droughts have also been intensifying in frequency and severity in Southern Africa as a whole, which has been attributed to climate variability (Chivangulula and Amraoui, 2024).

Wet years were also detected with the district experiencing regular moderate wet events (SPI between +0.4 to +1.2). From the current study, other years, 1941, 1929, 1947, 1959, and 1977, reflected mixed conditions, such as moderate wetness (+0.4 to +1.2) and while others recorded very wet conditions (SPI > +1.2). The year 2001 was identified as having extensive very wet conditions (SPI > +1.2). Similarly, historical rainfall analyses during the 20th century recorded numerous anomalously wet years in South Africa (McBride et al., 2022; Chivangulula and Amraoui, 2024).

Annual and seasonal VCI, VHI and TCI time series

The district experienced varying drought conditions with lower values in 2015 and 2018 in the ONDJFM season as reflected by the VCI, VHI and TCI annual and seasonal time series (Figure 5). These results are also consistent with the spatial analysis (Figures 4 and 6).

Spatiotemporal distribution of VCI, TCI, and VHI in ONDJFM season

Figure 6 shows the spatial distribution of TCI values, highlighting no droughts in years 2001, 2009 and 2022, while moderate to mild drought appear in 2005, 2012, 2015, and 2018. Small patches of extreme droughts are reflected in other environmental factors, such as, the topography, geographical site, and presence of warm and cold currents also influence the nature of extreme weather events across South Africa (Adelabu et al., 2025).

Similarly, patches of low VCI values reflecting severe drought were detected in 2018, 2015, 2012, 2005 (Figure 7). VCI analysis during the growing season is ideal in identifying the condition of crops with regards to moisture and vegetation health (Fentaw et al., 2023). VCI across the district reflect the drought severity through ONDJFM season when rainfall is critical for vegetation productivity. Drought occurrences during the growing season, that is, between September and November, may interrupt planting times and reduce germination rates, directly impacting the VCI values observed (Adelabu et al., 2025). Additionally, droughts in March coincide with critical crop reproductive and maturation stages, intensifying yield losses (Adelabu et al., 2025). Furthermore, the low rainfall, especially in 2015,

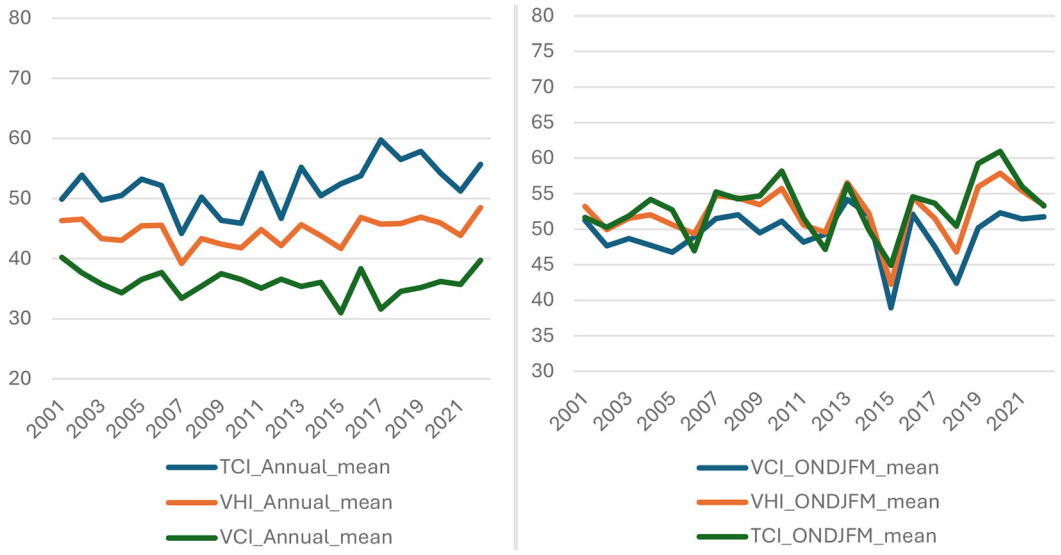

Figure 5. Trends in drought indices (VCI, TCI, VHI) from 2001 to 2022

probably resulted in a reduction in available soil moisture and retention, escalating drought impacts in areas undergoing severe conditions. A reduction in vegetation cover, soil erosion, surface runoff also leads to flooding becoming more pronounced (Hashemzadeh et al., 2022). Though SPI6 findings indicated the occurrence of widespread drought in 2018, irrigated or resilient vegetation areas of land recorded localized maximum VCI values in parts of the study

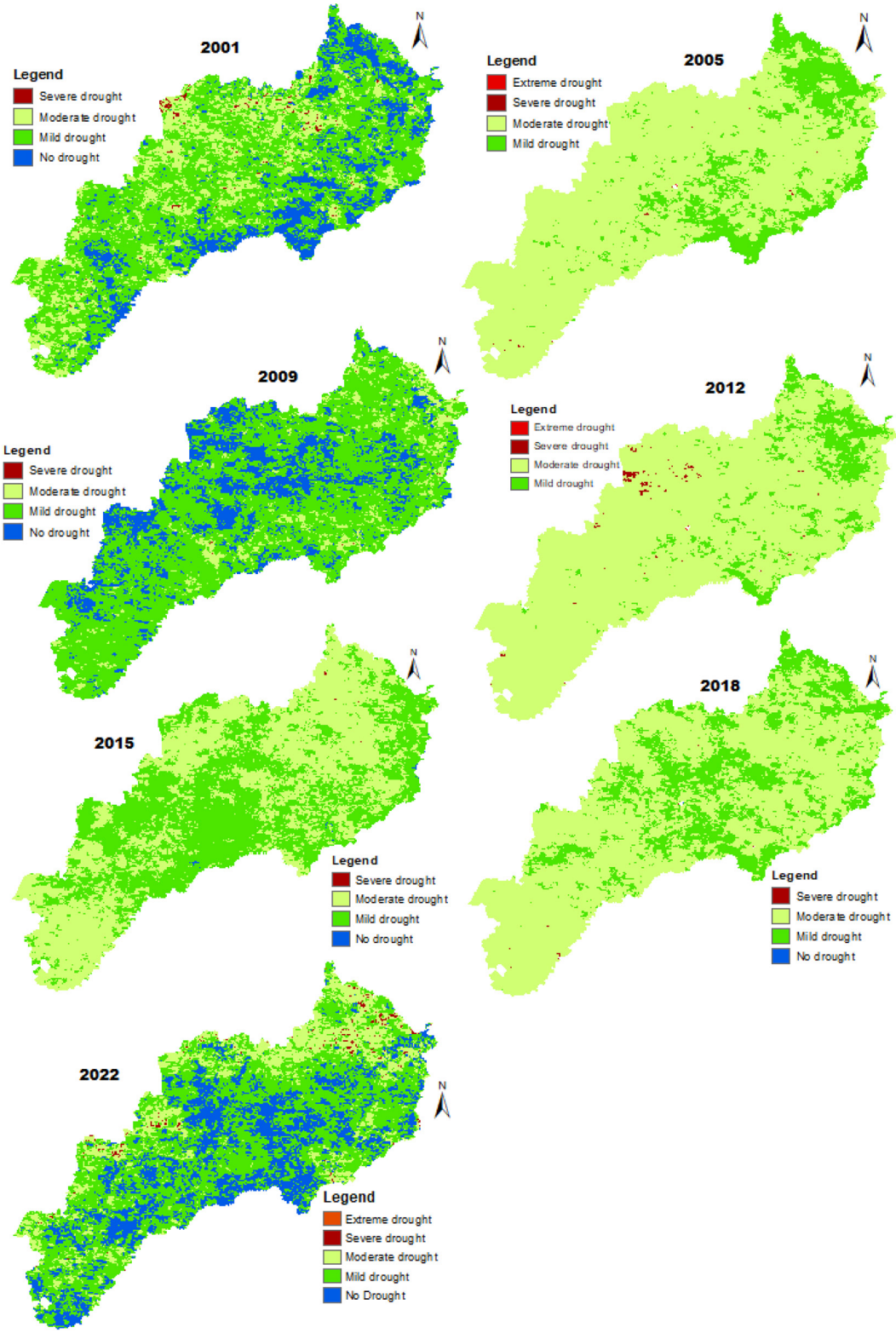

Figure 6. Drought mapping using TCI index from 2001–2022

area. This might indicate that climate and vegetation-based indices are thus complementary in nature since SPI values reveal rainfall anomalies and VCI captures vegetation conditions in both natural and man-made systems. Drought resistant crops provide local households with a coping mechanism against prevailing droughts (Ogundeji, 2022; Chisadza et al., 2025). In addition,, creating early warning systems and establishing access to climate information services

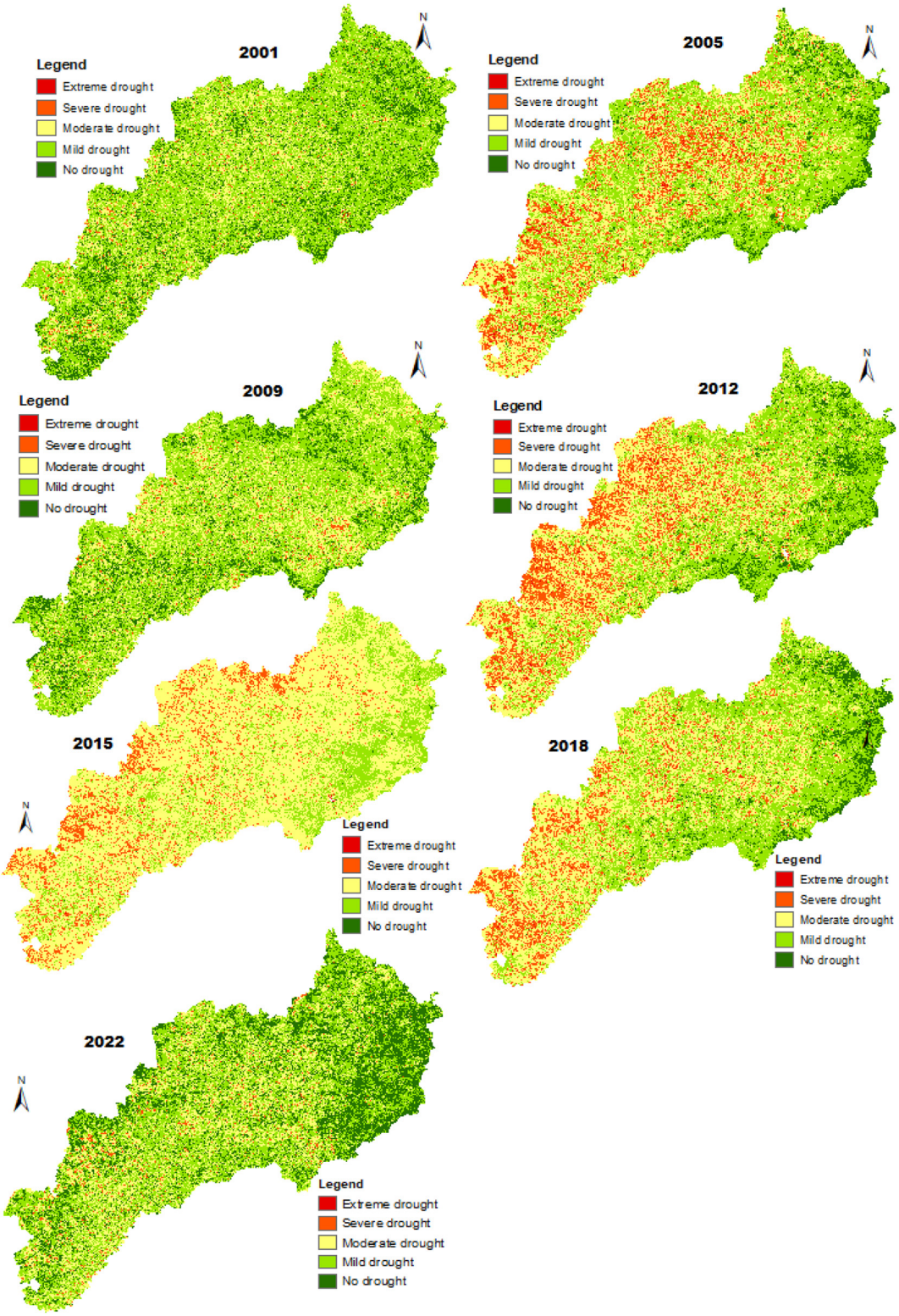

Figure 7. Drought mapping using VCI index from 2001–2022

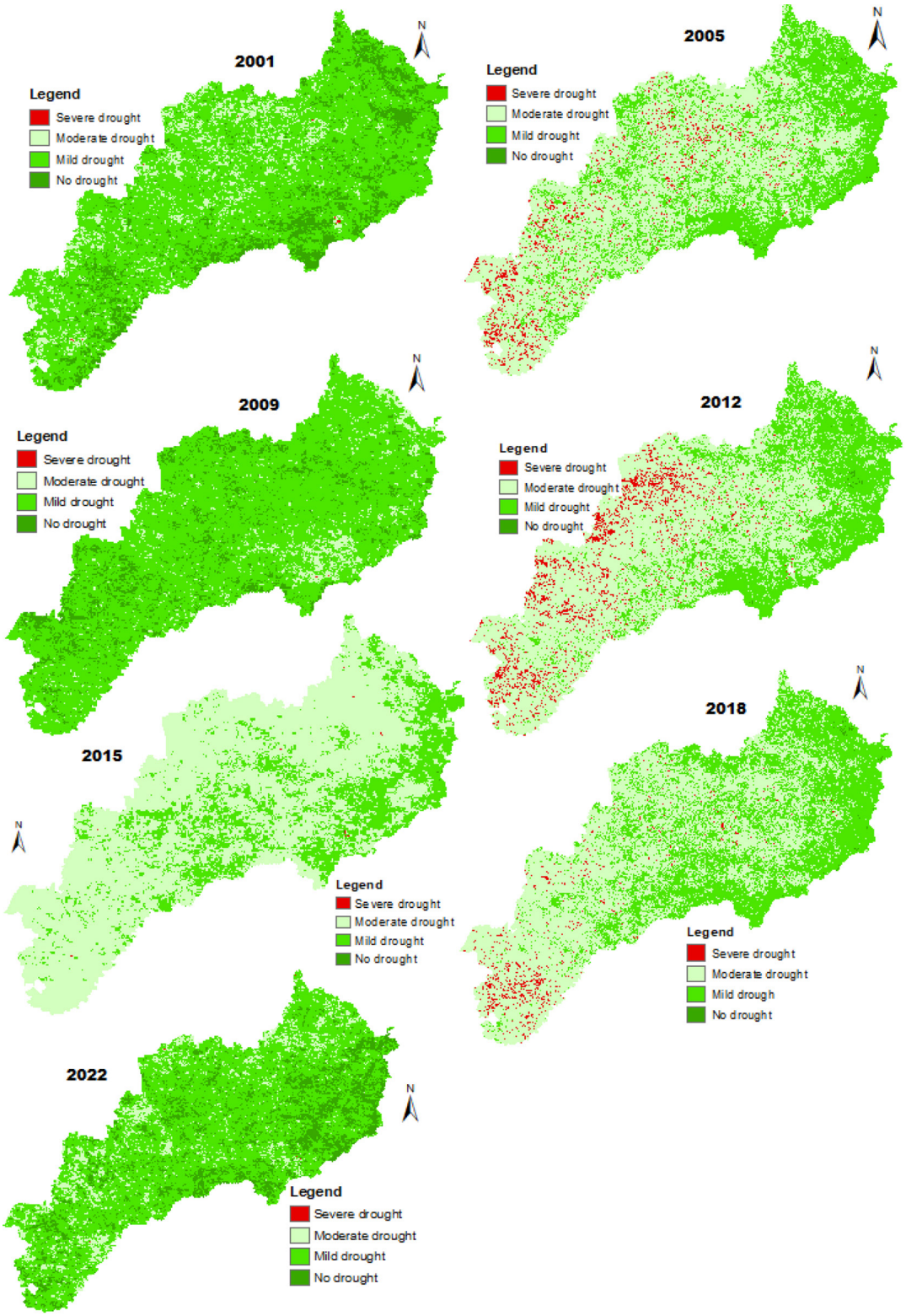

Figure 8. Drought mapping using VHI index from 2001–2022

would also undoubtably help communities with drought preparation and mitigating. All the indices in 2022, 2009 and 2001 spatially reflected no drought conditions.

The spatial analysis for VHI indices indicated that no droughts were identified in 2001, 2009 and 2022 (Figure 8). Moreover, high VHI values were observed in the eastern and south-eastern parts of the region. On the other hand, no extreme drought was detected using the VHI. However, some small areas recorded severe droughts in 2005, 2012 and 2018. VHI values did

Table 2. Results of Pearson's correlation between SPI-6 and vegetation indices in this study

Index1	Index2	r-value	p-value
EVI	SPI6	-0.073	0.748
EVI	TCI	0.703	0.000
EVI	VCI	0.749	0.000
EVI	VHI	0.807	0.000
SPI6	TCI	-0.210	0.348
SPI6	VCI	0.259	0.245
SPI6	VHI	0.048	0.833
TCI	VCI	0.604	0.003
TCI	VHI	0.886	0.000
VCI	VHI	0.902	0.000

not reveal widespread drought conditions similar to the SPI, but only reflected markedly dry conditions over the 2015–2016 drought period. Unlike SPI, which indicated widespread drought, VHI captured localized dry anomalies, particularly during the 2015–2016 drought period.

Correlation analysis

A correlation analysis was conducted and a summary of the correlation among the indices EVI, VCI, TCI, SPI6 and VHI is shown (Table 2). Correlation values measure the strength of a relationship between variables and fall between +1 and −1, where +1 is the extreme positive correlation value, whereas −1 reflects the extremely negative value (Vaishnavi, 2023). The findings from this study uncovered a strong positive correlation between VCI and VHI indicating a significant relationship between the two indices ($r = 0.902$, $p < 0.001$). Similarly, the influence of temperature on vegetation health is also revealed by a high correlation between VHI and TCI ($r = 0.886$, $p < 0.001$), confirming the influence of temperature on vegetation health. Moderate correlations were also observed between EVI and VCI ($r = 0.749$, $p < 0.001$) and between EVI and VHI ($r = 0.807$, $p < 0.001$).

On the contrary, weak correlations were exhibited between SPI6 and the vegetation indices, signifying the presence of more complex vegetation dynamics which cannot be explained by precipitation anomalies alone (e.g., SPI6–VCI $r = 0.259$, $p = 0.245$; SPI6–VHI $r = 0.048$, $p = 0.833$). This pattern emphasises the importance of highlighting the role of temperature and vegetation conditions in driving VHI which may have a greater influence on vegetation health than rainfall (Table 2). Lagged correlations between rainfall and vegetation indices were not assessed in this study, which remains a limitation and an important area for future research.

CONCLUSIONS

Thabo Mofutsanyane District is one of the most agriculturally productive regions in South Africa. Rainfall analysis revealed anomalously wet years and severe drought episodes across the century, many of which aligned with El Niño events. The SPI analysis (1906–2023) confirmed widespread droughts, with 2018 being the most extreme. Vegetation indices provided complementary insights into localized drought impacts, revealing both severe stress periods and resilience patterns that rainfall data alone could not capture. The drought indices revealed the occurrence of mild to severe drought across multiple years, with seasonal impacts during ONDJFM affecting crop germination and health. This study filled a significant gap in South Africa's mountainous areas by combining meteorological and vegetation-based indices to monitor drought on a district scale. The present study demonstrated that agricultural droughts in the Thabo Mofutsanyane District are becoming more frequent and spatially diverse, with certain regions preserving vegetation health despite significant rainfall deficits. Vegetation stress reacts more significantly to temperature and local vegetation conditions than to rainfall anomalies alone, underscoring the necessity of integrating multiple indices for precise drought evaluation. By integrating meteorological and vegetation-based indicators, the study provides a repeatable approach to identify drought magnitude, timing, and spatial variability, offering new insights into localized resilience and the complex climate vegetation interactions that drive agricultural vulnerability in semi-arid regions. These findings confirm that the study's goal was achieved, fill a critical gap in long-term district-scale drought monitoring, and open future directions for extending multi-index drought assessment to other semi-arid agricultural regions and diverse mountain environments.

REFERENCES

1. Adelabu, S., Durowoju, O. S., Adagbasa, E. G., Matamanda, A., Olusola, A. (2025). Footprints of drought in a montane grassland biome : a drought vulnerability index approach to drought conditions. *African Geographical Review*, *00*(00), 1–23. https://doi.org/10.1080/19376812.2025.2530636
2. Badasa, M., Biratu, M., Merga, B., Obsi, D. (2022). Multiple indices - based assessment of agricultural drought : A case study in Gilgel Gibe Sub - basin, Southern Ethiopia. *Theoretical and Applied Climatology*, 455–464. https://doi.org/10.1007/s00704-022-03962-4
3. Bahta, Y. T., Myeki, V. A. (2021). Adaptation, coping strategies and resilience of agricultural drought in South Africa: implication for the sustainability of livestock sector. *Heliyon*, *7*(11), e08280. https://doi.org/10.1016/j.heliyon.2021.e08280
4. Baudoin, M., Vogel, C., Nortje, K., Naik, M. (2017). Living with drought in South Africa : lessons learnt from the recent El Niño drought period. *International Journal of Disaster Risk Reduction*, *23*(May), 128–137. https://doi.org/10.1016/j.ijdrr.2017.05.005
5. Bento, A. (2018). Contribution of land surface temperature (TCI) to vegetation health index : A comparative study using. *Remote Sensing*, *10*, 1324. https://doi.org/10.3390/rs10091324
6. Bhowmik, S., Bhatt, B. (2024). *Drought Monitoring Using MODIS Derived Indices and Google Earth Engine Platform for Vadodara District, Gujarat*. 1885–1900.
7. Blamey, R. C., Kolusu, S., Mahlalela, P., Todd, M., Reason, C. J. (2018). The role of regional circulation features in regulating El Niño climate impacts over southern Africa: A comparison of the 2015 / 2016 drought with previous events. *International Journal of Climatology*, *38*(April), 4276–4295. https://doi.org/10.1002/joc.5668
8. Botai, C. M., Botai, J. O., Dlamini, L. C., Zwane, N. S., Phaduli, E. (2016). Characteristics of droughts in South Africa: A case study of free state and North West provinces. *Water (Switzerland)*, *8*(10). https://doi.org/10.3390/w8100439
9. Chisadza, B., Gwate, O., Peter, S., Mpofu, N., Macherera, M. (2025). Resilient agriculture in semi - arid Zimbabwe : adaptation strategies and influencers among smallholder farmers. *Discover Agriculture*. https://doi.org/10.1007/s44279-025-00234-3
10. Chivangulula, F. M., Amraoui, M. (2024). The drought regime in Southern Africa: Long - term space - time distribution of main drought descriptors. *Environmental Science, Geography* 1–28.
11. FAO. (2017). *FAO Southern Africa El Niño Response Plan (2016/17)*. Food and Agriculture Organization of the United Nations.
12. Fentaw, A. E., Yimer, A. A., Zeleke, G. A. (2023). Monitoring spatio-temporal drought dynamics using multiple indices in the dry land of the upper Tekeze Basin, Ethiopia. *Environmental Challenges*, *13*(July), 100781. https://doi.org/10.1016/j.envc.2023.100781
13. Hashemzadeh, M., Mehdi, G., Ali, V., Damavandi, A. (2022). Agricultural drought assessment using vegetation indices derived from MODIS time series in Tehran Province. *Arabian Journal of Geosciences*. https://doi.org/10.1007/s12517-022-09741-9
14. Hlalele, B. M. (2019). A multi-dimensional drought risk analysis in the Free State drought-hit municipalities, South Africa. *Eco. Env. & Cons.*, *25*(2), 968–974.
15. Kashyap, R., Kuttippurath, J., Patel, V. K. (2025). Ecological droughts increased in India with changing Indian summer monsoon and human interventions. *Commun Earth Environ*, 1–17.
16. Kganyago, M., Mukhawana, M.., Mashalane, M., Mgabisa, A., Moloele, S. (2021). Recent trends of drought using remotely sensed and in-situ indices: towards an integrated drought monitoring system for South Africa. *IEEE International Geoscience and Remote Sensing Symposium IGARSS*, *2021*, 6225–6228. https://doi.org/10.1109/IGARSS47720.2021.9554117
17. Kruger, A., Nxumalo, M. (2017). Historical rainfall trends in South Africa: 1921–2015. *Water SA*, *43*(2), 285–297. https://doi.org/http://dx.doi.org/10.4314/wsa.v43i2.12
18. Mathivha, F. I., Matimolane, S. (2025). Comparative assessment of standardised indices for monitoring drought in North-Eastern South Africa. In *Environmental Sciences. IntechOpen.* https://doi.org/10.5772/intechopen.1009745
19. Mazibuko, S. M., Mukwada, G., Moeletsi, M. E. (2021). Assessing the frequency of drought / flood severity in the Luvuvhu River catchment, Limpopo Province, South Africa. *WaterSA*, *47*(2), 172–184.
20. McBride, C. M., Kruger, A. C., Dyson, L. (2022). Changes in extreme daily rainfall characteristics in South Africa: 1921–2020. *Weather and Climate Extremes*, *38*(July), 100517. https://doi.org/10.1016/j.wace.2022.100517
21. Mckee, T. B., Doesken, N. J., Kleist, J. (1993). *The relationship of drought frequency and duration to time scales*. *January*, 17–22.
22. Msimanga, L., Mukwada, G. (2024). An assessment of the perceptions of local communities in the Eastern Free State Region of South Africa regarding the impacts of climate change on livelihoods An assessment of the perceptions of local commu. *Transactions of the Royal Society of South Africa*, *79:1*, 51–65. https://doi.org/10.1080/00359 19X.2024.2322939

23. Msimanga, L., Mukwada, G. (2025). Examining spatiotemporal trends of temperature and precipitation and households perceptions of climate change in the Eastern Free State Region of South Africa. *Advances in Meteorology*, *2025*(Article ID 7161645), 26. https://doi.org/10.1155/adme/7161645
24. Mukhawana, M. B., Kanyerere, T. (2023). Review of In-Situ and Remote Sensing-Based Indices and Their Applicability for Integrated Drought Monitoring in South Africa. *Water.*
25. Mukwada, G., Mutana, S. (2023). *Surviving the Limits Imposed by a Changing Climate: The Case of Urban Drought and Water Supply Sustainability in Phuthaditjhaba*. Springer International Publishing. https://doi.org/10.1007/978-3-031-15773-8_6
26. Muyambo, F., Belle, J., Nyam, Y. S., Orimoloye, I. R., Muyambo, F., Belle, J., Nyam, Y. S., Orimoloye, I. R. (2024). Climate change extreme events and exposure of local communities to water scarcity : a case study of QwaQwa in South Africa. *Environmental Hazards ISSN:*, *23:5*, 405–422. https://doi.org/10.1080/17477891.2024.2315263
27. Nabizada, M. J., Köylü, Ü. (2025). Comparative analysis of multi-sensor integrated indices for agricultural drought monitoring during the monsoon season in the Helmand River Basin, Afghanistan. *Theoretical and Applied Climatology*, *156*, 214. https://doi.org/10.1007/s00704-025-05432-z
28. Ncube, B. (2017). *Coping and adaptation strategies for agricultural water use during drought periods.* (Issue May).
29. Ngwenya, S. J., Mukwada, G. (2024). Impacts of climate hazards on households along the Drakensberg Mountains in the Free State Province of South Africa. *GeoJournal*, *89: 66*, 1–17. https://doi.org/10.1007/s10708-024-11061-2
30. Ogundeji, A. A. (2022). Adaptation to climate change and impact on smallholder farmers' food security in South Africa. *Agriculture (Switzerland)*, *12*, *589.* https://doi.org/https://doi.org/10.3390/ agriculture12050589 Academic
31. Onyeuwaoma, N. (2024). Modelling drought in South Africa : meteorological insights and predictive parameters. In *Environmental Monitoring and Assessment* (Vol. 196, Issue 10). Springer International Publishing. https://doi.org/10.1007/s10661-024-13009-y
32. Orimoloye, I. R., Zhou, L., Kalumba, A. M. (2021). Drought disaster risk adaptation through ecosystem services-based solutions: Way forward for south africa. *Sustainability (Switzerland)*, *13*(8). https://doi.org/10.3390/su13084132
33. Pavlidis, V., Kganyago, M., Mukhawana, M., Alexandridis, T., Cherif, I., Laneve, G., Orsi, R., Kartsios, S., Karypidou, M. C., Sofiadis, I., Katragkou, E. (2024). A drought monitoring and early warning service for food security in South Africa. *Climate Services*, *34*(January), 100463. https://doi.org/10.1016/j.cliser.2024.100463
34. Rahimabadi, Dehghan, P., Abdolshahnejad, M., Alamdarloo, Esmail, H., Azarnivand, H. (2024). Vegetation dynamics assessment: Remote sensing and statistical approaches to determine the contributions of driving factors. *Journal of the Indian Society of Remote Sensing*, *52*, 1969–1984. https://doi.org/doi.org/10.1007/s12524-024-01917-y
35. Reason, C., Jagadheesha, D. (2014). A model investigation of recent ENSO impacts over southern Africa. *Meteorology and Atmospheric Physics*, *89*(January 2005), 181–205. https://doi.org/10.1007/s00703-005-0128-9
36. Rouault, M., Reason, C., Lutjeharms, J. R., Mulenga, H., Richard, Y., Fauchereau, N., Trzaksa, S. (2003). *Role of the Oceans in South Africa'S Rainfall* (Issue 953).
37. Statistics South Africa, 2025. (2023). *Poverty trends in South Africa An examination of absolute poverty between 2006 and 2023*. Statistics South Africa. https://doi.org/https://www.statssa.gov.za/
38. Tshabalala, K. (2023). *Characterisation of Drought Using Hydrological and Meteorological Indices: A Case Study of Bethlehem, South Africa* (Issue 1597540). University of the Witwatersrand.
39. Vaishnavi, M. K. D. K. (2023). Dynamic drought risk assessment and analysis with multi - source drought indices and analytical hierarchy process. *International Journal of Environmental Science and Technology*, *20*(3), 2839–2856. https://doi.org/10.1007/s13762-022-04041-x
40. Van Niekerk, J., Conradie, B. (2023). Cereal production in the eastern free state, 1981–2007: can agricultural extension deliver food security? *South African Journal of Agricultural Extension*, *51*(2), 68–88. https://doi.org/10.17159/2413-3221/2023/v51n2a14653
41. Wolski, P. (2018). How severe is Cape Town's "Day Zero" drought? *Significance*, *15*(2)(April), 24–27. https://doi.org/10.1111/j.1740-9713.2018.01127.x
42. Wolski, P., Jack, C., Tadross, M. (2020). Spatio-temporal patterns of rainfall trends and the 2015 – 2017 drought over the winter rainfall region of South Africa. *Int J Climatology*, *July*, 1–17. https://doi.org/10.1002/joc.6768
43. Wyss, D., Negussie, K., Staacke, A., Karnagel, A., Engelhardt, M., Kappas, M. (2022). A comparative analysis of MODIS-derived drought indices for Northern and Central Namibia. *African Journal of Environmental Science and Technology*, *16*(May), 173–191. https://doi.org/10.5897/AJEST2022.3096